

Article

# Integrated Underwater Detection and Communication System Based on P4 Code-Modulated OFDM Signal

Xinglong Feng<sup>1</sup>, Zhenyi Zhao<sup>1</sup>, Yuzhong Zhang<sup>1</sup> and Qiao Hu<sup>1,2,\*</sup> 

<sup>1</sup> School of Mechanical Engineering, Xi'an Jiaotong University, Xi'an 710049, China; fengxinglong@stu.xjtu.edu.cn (X.F.); zzyxjtu@stu.xjtu.edu.cn (Z.Z.); zyz\_black@stu.xjtu.edu.cn (Y.Z.)

<sup>2</sup> Shaanxi Key Laboratory of Intelligent Robots, Xi'an Jiaotong University, Xi'an 710049, China

\* Correspondence: hqxjtu@xjtu.edu.cn

**Abstract:** Because of the requirements of marine resources exploration and underwater cooperative operation, the underwater operation of common detection and communication equipment is difficult and unreliable. Therefore, it is urgent to establish an accurate underwater target detection and multi-node communication integrated system. An integrated method of underwater electric field detection and communication based on P4 code-modulated OFDM signal is proposed in response to the above requirements. The working principle, system structure, and signal processing of underwater electric field detection and electric field communication are similar. This article uses detection signal P4 code to modulate the phase of OFDM communication signal, thus realizing the integration of Underwater Detection and Communication System (IUDCS). The simulation results show that IUDCS can meet the detection range and velocity characteristics of underwater dynamic targets. The simulation results also meet the requirements for communication error rate and symbol error rate, thereby verifying the performance of underwater electric field IUDCS. This method is necessary for the realization of IUDCS in terms of reducing platform size, reducing power consumption, and enhancing concealment. Moreover, it shows good application prospects in underwater robot cluster operations.

**Keywords:** orthogonal frequency division multiplexing; P4 code; phase modulation; detection and communication integration



**Citation:** Feng, X.; Zhao, Z.; Zhang, Y.; Hu, Q. Integrated Underwater Detection and Communication System Based on P4 Code-Modulated OFDM Signal. *J. Mar. Sci. Eng.* **2023**, *11*, 920. <https://doi.org/10.3390/jmse11050920>

Academic Editor: Yassine Amirat

Received: 14 March 2023

Revised: 19 April 2023

Accepted: 24 April 2023

Published: 25 April 2023



**Copyright:** © 2023 by the authors. Licensee MDPI, Basel, Switzerland. This article is an open access article distributed under the terms and conditions of the Creative Commons Attribution (CC BY) license (<https://creativecommons.org/licenses/by/4.0/>).

## 1. Introduction

With the increasing shortage of land resources, the development of marine resources is urgent. It has become a new field of global economic and defense strength competition. The ocean occupies 71% of the earth's surface and contains rich oil and gas resources, biological resources, and mineral resources. However, the harsh natural conditions hinder the exploration of the ocean. So far, human research on the oceans has mainly relied on space-based observation, underwater ocean observation, sea-based observation, and other means. Research and development of exploration tools have become a new direction for researchers. The complex underwater environment makes it difficult for ordinary detection equipment to conduct underwater detection. Moreover, the widely used communication methods on land also severely attenuate underwater. Therefore, it is very important to achieve precise detection of targets in complex underwater working environments and ensure smooth information exchange between underwater swarm robots. The content of this article is inspired by the electric field detection and communication mechanism of weakly electric fish in a complex underwater environment.

In underwater electric field detection, many teams have carried out relevant research and made some achievements in the field positioning in recent years. The random walk and minimum particle expected variance algorithm, proposed by Solberg et al. [1], and the Kalman filter algorithm, proposed by Lebastard et al. [2], have achieved a good positioning effect. Morel et al. also improved the underwater target location algorithm based on the

neural networks according to the optimization theory [3], improving the target location accuracy. Lanneau et al. [4] proposed an underwater target location method based on a multi-signal classification algorithm. Lim et al. [5] proposed a generalized MUSIC algorithm for underwater target location, which involves multiple inverses of the covariance matrix, resulting in relatively high computational complexity. Peng Jiegang and others from the University of Electronic Science and Technology proposed a simulation method for an active electric field positioning system based on a quasi-static electric field and the Cole–Cole resistivity model. It obtained the response laws of various materials of the target to underwater electric fields under different wave excitation signals [6]. At the same time, the developed underwater target positioning system requires less accuracy of the forward model. It approaches the target and locates the target through continuous iterative calculation and feedback motion [7]. At present, the commonly used target location algorithm is the moving location method based on the optimization theory, which has the disadvantages of slow search speed, large amount of computation, and poor location accuracy.

The field of underwater electric field communication has seen relatively little research due to the short communication distance of underwater electric fields. It was not until the early 21st century that electric field communication was re-studied as the exploration of the ocean deepened. Tucker et al. first proposed the concept of conducting electric field signals to realize the transmission and detection process of electric field communication signals [8]. Momma et al. [9], through the principle of recent communication, found that the effective distance of electric field communication is a function of current and verified the feasibility of electric field communication through experiments. Joe et al. [10] established the experimental transmission circuit of a quasi-static current field digital signal. They proposed a method to focus the current in the required direction to improve the underwater communication distance. The team also established a distance–frequency dependent path loss model, and the results of channel characteristics have important reference values for the design of digital communication [11]. Xie Guangming of Peking University has built a current communication system for a small bionic underwater vehicle, and analyzed the factors that influence the communication performance of key parameters such as electrode spacing and emitter current [12]. A team also designed the operation mechanism of the protocol and the detection method of channel status for the electric field communication of multiple robotic fish based on CSMA/CA [13]. Research teams at home and abroad have mainly carried out research on the factors affecting the communication performance of underwater electric fields, and the possibility of communication is only available at close range. To resist environmental interference in the actual use process, it is necessary to study a new modulation and demodulation technology and realize the multi-node cluster communication of underwater vehicles in engineering.

The advantages of underwater electric field communication in close-range communication include the following: (1) Due to changes in seawater temperature or density, as well as reflections and refractions caused by obstacles, there are problems with multipath effects and blind spots in underwater acoustic communication. In areas with obvious layered seawater media, communication is often difficult. There are no such problems with electric field communication, and the transmission signal is stable, i.e., not suddenly interrupted due to seawater stratification. (2) The absorption, emission, and refraction of electromagnetic waves by seawater are relatively large, and the higher the frequency, the greater the attenuation. Communication is often difficult in high-density areas. (3) Compared to underwater acoustic communication, underwater electric field communication is a low-noise system. In principle, increasing current without increasing power can expand the effective communication range. (4) The electric field communication method not only achieves wireless communication but also eliminates the need to install large antennas, making it simple and highly flexible [14–16]. The comparison of underwater electromagnetic waves, acoustic waves, and electric field communication is shown in Table 1.

**Table 1.** Comparison of electromagnetic waves, acoustic waves, and electric fields.

Characteristic	Electromagnetic Wave	Acoustic Wave	Electric Field
Media dependency	No need to rely on media	Must rely on medium vibration	Low medium dependency
Typical operating frequency	Megahertz	Tens of kilohertz	Tens of kilohertz
Absorption attenuation in water	3 dB/m@ 10 kHz	1.1 dB/km@ 10 kHz	Almost no attenuation
Media uniformity	Basically propagating in a straight line	Highly affected by temperature and propagated in a curved manner	Can achieve omnidirectional dissemination now
Propagation delay	Low latency	Large latency	Almost no latency
Communication distance	A few meters	Dozens of kilometers	Tens of meters
Affected by environmental factors	Electromagnetic noise impact	Emission, multipath impact	Electromagnetic noise impact

The discovery of weakly electric fish brings a new idea for integrating underwater target detection and cluster communication [17,18]. The weakly electric fish can emit a weak electric field through the discharge organs at the tail. When there are objects around, the electric field will be distorted. The weakly electric fish can sense the distorted electric field through the tissues on the body surface to achieve the goal of exploring the surrounding environment and the purpose of information interaction between the same species [19–21]. By actively transmitting and sensing electric field information, weakly electric fish can navigate, prey, communicate, and survive in the deep sea, which is completely dark and has no light, with bad and turbid water quality and a complex water environment. The advantages of using an active electric field for underwater detection and communication grant it unique performance advantages in adapting to complex water conditions with low visibility and turbidity. Weakly electric fish can actively generate the electric field and perceive the distortion of electric field so as to realize the target perception of the surrounding environment and the same kind of information interaction. Active electric field detection and electric field communication are related in the working principle, system structure, signal processing and other aspects. Therefore, research on integrating underwater electric field detection and communication system based on the OFDM mechanism of P4 code modulation is carried out [22,23].

In this article, the integration method of underwater electric field detection and communication based on P4 code-modulated OFDM signal is adopted to solve the difficulties of the integration of underwater electric field detection and communication. OFDM is a special multi-carrier transmission technology, which converts high-speed serial data into low-speed parallel sub-data streams and then modulates the data to multiple orthogonal sub-carriers for transmission. OFDM can effectively improve the frequency spectrum utilization, and by inserting guard intervals between OFDM symbols, the inter-channel interference and inter-symbol interference can be eliminated to a greater extent. P4 code has the fuzzy distance function, which has the characteristics of a narrower main lobe, lower side lobe, and better performance. The characteristic of the P4 code makes the modulated OFDM signal fuzzy function ideal, and it can easily realize the integration of the detection and communication systems. Therefore, this article adopts an underwater electric field detection and communication system integration based on P4 code-modulated OFDM mechanism. This article completes the simulation and validation of underwater IUDCS and prospects the potential application of the proposed method in underwater robot cluster operation.

The rest of this article is organized as follows: in Section 2, the P4 code modulate-OFDM detection and communication integration process is described; we complete the

simulation parameter setting and corresponding simulation result analysis of the integrated system of underwater electric field detection and communication in Section 3; Section 4 gives the simulation conclusion.

## 2. P4 Code-Modulated OFDM Detection and Communication Integration Process

### 2.1. OFDM Process

In order to overcome the influence of frequency selectivity of the broadband channels on single-carrier transmission, a multi-carrier can be used to achieve high data rate transmission. At the transmitter, pluralities of narrow-band filters decompose the broadband signal into several narrow-band signals. At the receiver, multiple narrow-band filters are used to synthesize these narrow-band signals [24].

The general form of the OFDM signal can be expressed as follows:

$$s(t) = \sum_{n=1}^N \omega_n \exp(j2\pi\Delta f t) u_n(t/T_b), \tag{1}$$

where  $N$  represents the number of subcarriers,  $\omega_n$  is the weighting coefficient of the  $n$  subcarrier, the OFDM symbol period is  $T_b$ ,  $u_n(t/T)$  is the rectangular envelope of the  $n$ th subcarrier data,  $\Delta f$  is the frequency interval of the subcarrier, and  $T\Delta f = 1$ . It can be seen that  $s(t)$  is a linear superposition of  $N$  single-frequency signals.

In an OFDM symbol period,  $T_b$ , each subcarrier contains an integer period—that is, the single period length of the  $n$ th subcarrier is  $T_b/n$ —and each adjacent subcarrier has a period difference, then:

$$\frac{1}{T_b} \int_0^{T_b} \exp(j2\pi f_n t) \exp(-j2\pi f_m t) dt = \begin{cases} 1 & m = n \\ 0 & m \neq n \end{cases} \tag{2}$$

Each subcarrier sequence is sending its own signal, overlapping each other in the medium and finally seeing the signal at the receiver is  $f(t)$ . After receiving the hybrid signal  $f(t)$ , the receiver performs the operation of multiplication and integration on each subcarrier, respectively; then, the signals carried by each subcarrier can be taken out, respectively. The OFDM system in the time domain is shown in Figure 1.

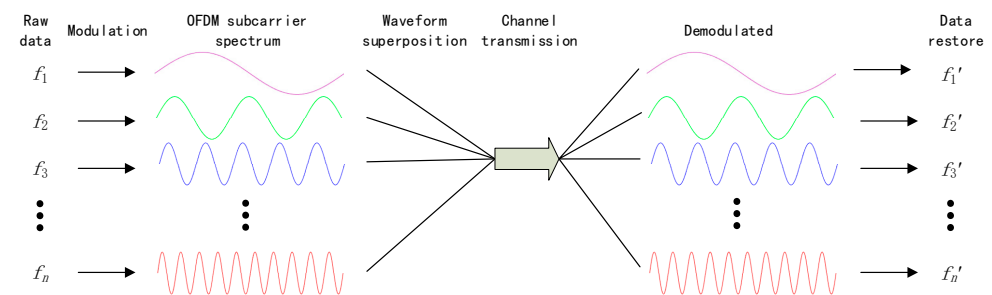
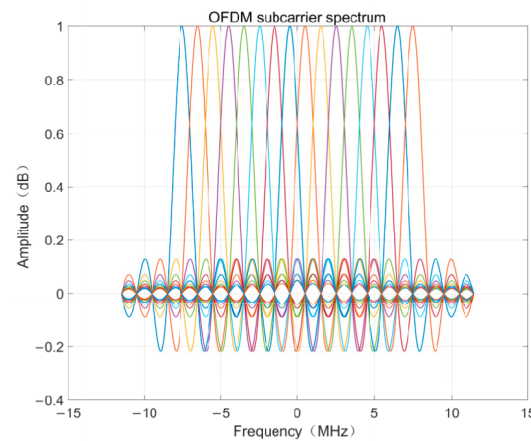


Figure 1. Schemes follow the same formatting.

From the analysis in the frequency domain, the multiplication of the time domain in  $s(t)$  corresponds to the convolution in the frequency domain. The spectrum amplitude of the known rectangular pulse is the  $\text{sinc}(fT_b)$  function, which has the maximum value at  $f = 0$  and is zero at the frequency points at integer multiples of  $1/T_b$ . The spectrum of OFDM subcarriers is shown in Figure 2, and the frequency interval of adjacent orthogonal sub-carriers is  $\Delta f$ . Since the subcarrier interval is at the maximum value of a subcarrier, the maximum value of the spectrum of each subcarrier is calculated during demodulation. At this time, only the subcarrier has a signal. As long as the maximum point is aligned, the symbol of each subchannel can be extracted from the overlapping sub-channels without interference from other subchannels [25].



**Figure 2.** Spectrum diagram of OFDM subcarrier.

### 2.2. P4 Code-Modulated OFDM Signal

Phase-coded signals have high similarity with OFDM signals, and the angle analysis of communication shows that the phase coded signal is similar to MPSK modulation. For the detection system, the sum of multiple phase-coded detection signals with different frequencies is the OFDM phase-coded signal, so the spectrum of the signal will be relatively wide [26]. The polyphase coding characteristics of P4 code modulation are analyzed below.

P4 code is a common multiphase code used in detection. Its generation principle is Nyquist sampling based on the real and imaginary parts of the baseband LFM signal. P4 code takes the center frequency of the LFM signal as the local frequency, so the region with the most phase growth of P4 code is at both ends of the encoding, so it has a good bandwidth limit tolerance, which is conducive to reducing out-of-band noise superposition [27]. The phase increment of the P4 code is:

$$\phi_m = \frac{\pi(m - 1)^2}{N_p} - \pi(N_p - 1), \tag{3}$$

where  $m = 1, 2, 3, \dots, N_p$ ,  $N_p$  representing P4 code bits, and  $\phi_m$  is the phase jump coefficient. P4 code essentially comes from the sampling of the linear frequency modulation signal, so it still retains excellent Doppler tolerance in terms of detection performance. It is suitable for application in the scenario where the detection target has relative speed.

The characteristics of the P4 code make the fuzzy function of the OFDM signal ideal, and OFDM signal has the features of multi-carrier transmission. Therefore, an integrated signal of detection and communication based on cyclic shift P4 code is designed. For integrated detection and communication systems, the echo of the integrated transmission signal received by the receiver of the system is processed through the accumulation of pulses. When the cumulative number of pulses increases, the cyclically shifted P4 code can still maintain good ambiguity function characteristics and anti-Doppler ability, and it has good autocorrelation characteristics [28].

The autocorrelation function of the 32-bit P4 code is simulated and analyzed. As shown in Figure 3, the autocorrelation performance of 32-bit P4 code is relatively good, which can effectively reduce the adverse impact of communication information modulation on the ambiguity function of the integrated waveform. It is beneficial to the detection and communication integration of echo signal identification [29,30].

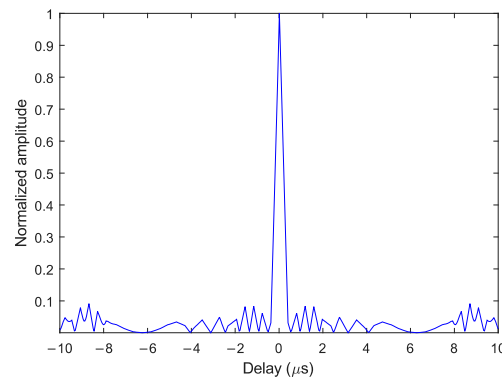


Figure 3. Autocorrelation function of 32-bit P4 code.

The 32-bit P4 code ambiguity function is shown in Figure 4. The results show that the ambiguity function is in the shape of a diagonal blade. Its important feature is that the fuzzy volume is concentrated on the “ridge” that coincides with the axis. The narrow pulse is oriented along the frequency axis and has good range resolution. The wide pulse is oriented along the time delay axis and has good velocity resolution.

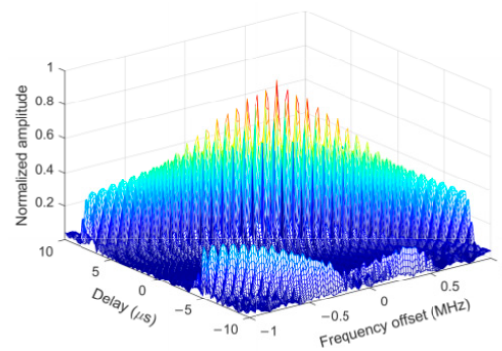


Figure 4. Ambiguity Function of 32-bit P4 Code.

The chip of OFDM corresponds to the communication symbol.  $c_m$  is the sequence number after bit mapping and the corresponding phase state, which can be regarded as a decimal number. Therefore, the phase on each OFDM subcarrier is determined by the number of  $c_m$  and P4 codes.  $c_m$  can represent the shift of P4 codes, so different communication information can be represented by different shift orders. Figure 5 shows the carrying process of 32-bit cyclic shift P4 code communication information.

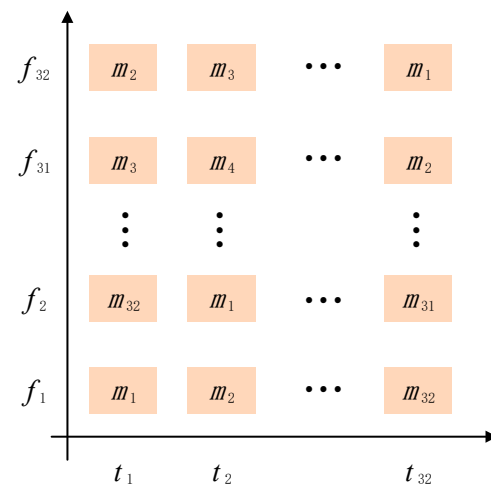


Figure 5. Communication information modulation of 32-bit cyclic shift P4 code.

### 2.3. Integration Process of Detection and Communication System Based on OFDM Mechanism of P4 Code Modulation

The signal of the integration process of detection and communication system based on the OFDM mechanism of P4 code modulation is expressed as:

$$s(t) = \sum_{n=0}^{N-1} \sum_{m=0}^{M-1} h_{m,n} e^{j2\pi n \Delta f (t - mT_b)} \text{rect}\left(\frac{t - mT_b}{T_b}\right), \tag{4}$$

where  $M$  is the number of OFDM symbols,  $N$  is the number of subcarriers,  $T_b$  is the width of an OFDM subcarrier symbol,  $\Delta f = 1/T_b$  is the subcarrier frequency interval,  $h_{m,n}$  represents the communication data information loaded on the  $m$ th symbol of the  $n$ th subcarrier of OFDM, and it is an  $N \times M$  matrix. In the matrix, each column vector represents an OFDM symbol, each row vector represents an OFDM subcarrier, and each element represents the complex data made from binary data by a cyclic shift of P4 code. The time-frequency structure of P4 code-modulated OFDM detection and communication integration signal is shown in Figure 6:

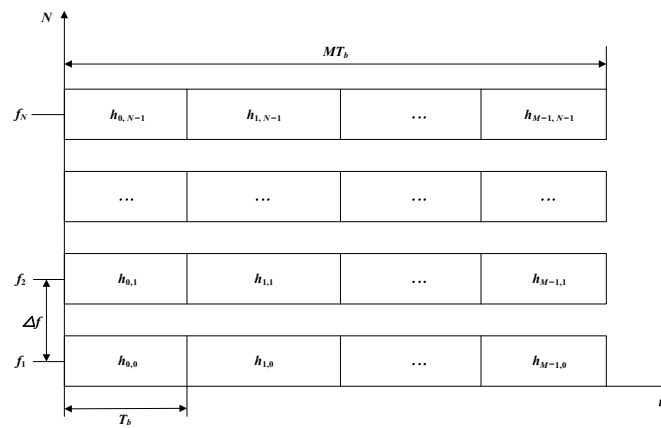


**Figure 6.** Time-frequency structure of P4 code-modulated OFDM detection communication integrated signal.

As shown in Figure 6, when the number of subcarriers is  $N$ , and the number of OFDM symbols is  $M$ , a maximum of  $N \times M$  modulation data can be transmitted within a pulse. Bandwidth  $B$  of OFDM shared signal is determined by the number of subcarriers  $N$  and the frequency interval  $\Delta f$ . It is expressed as:

$$B = N \Delta f. \tag{5}$$

The signal duration is determined by the number of OFDM symbols  $M$  and the duration of an OFDM symbol  $T_b$ :

$$T_s = MT_b. \tag{6}$$

According to the orthogonal characteristics of the integrated signals, it can be known that the time–bandwidth product  $P$  of OFDM detection signals in the shared system is:

$$P = BT_s = NM. \tag{7}$$

It can be seen that the integrated signal brings the characteristics of the large time–bandwidth product, and the detection has a high resolution.

After a series of processing at the receiver, the signal entering the detection processing module is expressed as:

$$y(t) = \sum_{n=0}^{N-1} \sum_{m=0}^{M-1} h_{m,n} e^{j2\pi f_c \frac{2R}{c}} e^{j2\pi n \Delta f (t - mT_b - \tau(t))} e^{j2\pi f_d t} \text{rect}\left(\frac{t - mT_b - \tau(t)}{T_b}\right) + n_p(t), \tag{8}$$

where  $R$  represents the distance between the detection and communication integration platform and the target to be measured,  $\nu$  represents the target moving speed,  $f_c$  represents the carrier frequency,  $c$  represents the transmission speed of the underwater electric field,  $\tau(t) = (2R - 2\nu t)/c$  represents the delay of the echo signal,  $f_d = 2\nu f_c/c$  represents the Doppler frequency shift, and  $n_p(t)$  represents the noise.

According to Equation (8), FFT demodulation of the target echo signal can be obtained:

$$g(f) = \frac{1}{2} T_b \sum_{n=0}^{N-1} \sum_{m=0}^{M-1} h_{m,n} e^{-j\pi n \Delta f T_b} e^{-j2\pi f (mT_b - T_b/2)} \text{sinc}(\pi(f - n\Delta f)T_b). \quad (9)$$

The communication terminal uses a constant envelope OFDM signal to reduce PAPR, and the bit error rate of the constant envelope OFDM system is analyzed [31–33]. The receiving signals at the receiver are:

$$r(t) = s(t) \exp\{j\varphi_0\} + w_t, \quad (10)$$

where  $\varphi_0$  is the additional frequency shift of the channel, and  $w_t$  is the noise signal, assuming that the noise received is the Gaussian white noise signal.

Therefore, the expression of the signal after phase demodulation is:

$$\phi'(t) = \phi(t) + \varphi_0 + \theta + \zeta(t), \quad (11)$$

where  $\theta$  is the additional phase shift of the phase demodulation, and  $\zeta(t)$  is the nonlinear output of Gaussian white noise, meeting the following requirements:

$$\zeta(t) = \arctan \left[ \frac{A_w(t) \sin[\phi_w(t) - \phi(t) - \theta - \varphi_0]}{A + A_w(t) \sin[\phi_w(t) - \phi(t) - \theta - \varphi_0]} \right] \quad (12)$$

where  $A_w(t)$  and  $\phi_w(t)$  are the amplitude and phase information of the noise.

The integrated signal of OFDM underwater electric field detection and communication based on P4 code modulation can be used to analyze the speed and distance of the target by the pulse compression algorithm, as well as the information sent by FFT demodulation. The integrated block diagram of integration of the detection and communication system based on the OFDM mechanism of P4 code modulation is shown in Figure 7 [34,35].

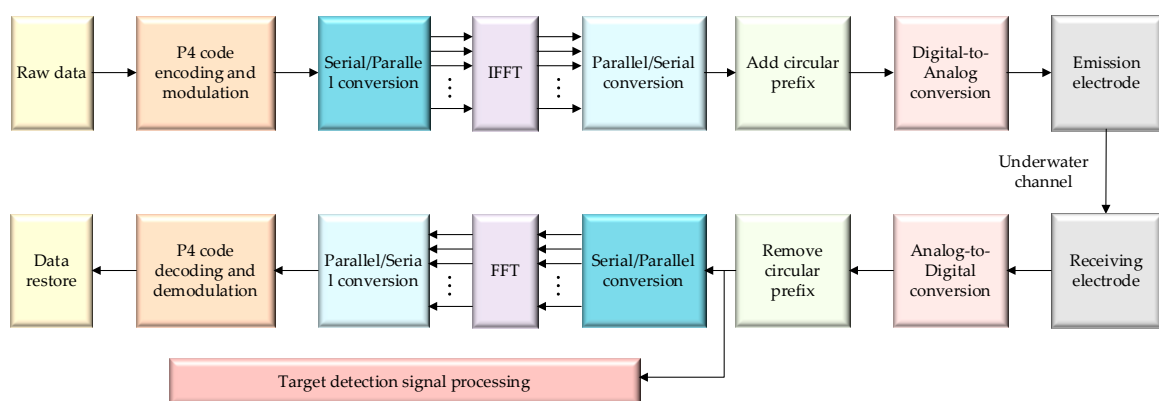


**Figure 7.** Block diagram of integration of detection and communication system based on OFDM mechanism of P4 code modulation.

The system first generates binary data at the transmitter, encoding and modulating the communication information data into P4 code sequence. The modulated data are converted into multi-channel low-speed data through series-to-parallel and then IFFT in the digital domain and converted into the serial data stream after parallel-to-serial conversion. Then, after adding the cyclic prefix and D/A conversion, it is transmitted through the transmitting electrode through the channel. At the receiver, after A/D conversion

and removing the cyclic prefix, the signal is sent to the communication signal processing module and the detection signal processing module, respectively. After the communication information passes the series to parallel conversion, FFT, and parallel-to-serial conversion, the phase information of the P4 code is obtained after the demodulation and decoding mode is completed, and the communication data are restored, while the detection and processing module carries on the multi-target signal processing so as to extract the target information and complete the speed and ranging measurement function. P4 codes can form complementary sets through cyclic shifts, representing different communication information through different shift orders, thus achieving information encoding and decoding. The whole system is based on the principle of underwater electric field detection and communication, which can realize the sharing of the integrated platform of detection and communication system.

### 3. Integrated Simulation of Detection and Communication

#### 3.1. Simulation Parameter Setting

The signal transmission model used in this article is a quasi-static electric field channel model. When the changing current flows through the emission electrode, the alternating electromagnetic field will be generated nearby, and the transmission medium, water, is a good conductor, so the conduction current and displacement current effect must be considered at the same time. The goal of simplification is to analyze the physical model of electric field communication by analyzing multiple electrostatic field sequences with varying field strengths over time; that is, the alternating electric field satisfies quasi-static field conditions if we set the simulation parameters as below.

For the simulation environment in seawater,  $\sigma$  is the conductivity,  $\mu$  is the permeability, and  $f$  is electrode transmission frequency. When  $\sigma = 4$ ,  $\mu = 1.257 \times 10^{-6} \text{ Hm}^{-1}$ ,  $f = 12 \text{ kHz}$ , the propagation wavelength of the electric field in seawater can be expressed as:

$$\lambda = \frac{2\pi}{\sqrt{\pi f \mu \delta}} = 14.431 \text{ m}, \tag{13}$$

Underwater electric field transmission wave speed is  $v$ , the unit of frequency—can be configured by the user through the “frequency” property.

$$v = \lambda f = 1.732 \times 10^5 \text{ m/s} \tag{14}$$

We set the bandwidth  $B = 100 \text{ kHz}$ , IFFT, and FFT point  $N_f$  to 1024, and carrier number  $N = 1024$ .

The carrier interval is:

$$\Delta f = B/N = 97.656 \text{ Hz}. \tag{15}$$

The maximum majority Doppler shift is:

$$fd_{max} = \Delta f/10 = 9.7656 \text{ Hz}. \tag{16}$$

OFDM period  $T_b$  is:

$$T_b = 1/\Delta f = 0.0102 \text{ s}. \tag{17}$$

Distance resolution is:

$$R_{max} = c * T_b/2 = 886.784 \text{ m}. \tag{18}$$

The velocity resolution is:

$$V_{max} = c * fd_{max}/f/2 = 70.4753 \text{ m/s}. \tag{19}$$

Table 2 shows the parameter setting for underwater electric field IUDCS simulation. Under these parameters, the detection performance and communication performance of the integrated detection and communication system are simulated and analyzed.

**Table 2.** Settings of the system simulation parameter.

Symbol	Parameter	Value
$\sigma$	Conductivity	$4 \text{ Sm}^{-1}$
$\mu$	Permeability	$1.257 \times 10^{-6} \text{ Hm}^{-1}$
$f$	Transmission frequency	12 kHz
$\lambda$	Wavelength	14.431 m
$v$	Wave velocity	$1.732 \times 10^5 \text{ m/s}$
$B$	Bandwidth	100 kHz
$N_f$	IFFT and FFT points	1024
$N$	Number of subcarriers	1024
$\Delta f$	Carrier interval	97.656 Hz
$M$	Number of OFDM	256
$T_b$	OFDM period	0.0102 s
$Q$	Number of data in an element period	1
$fd_{max}$	Maximum Doppler shift	9.7656 Hz
$R_{max}$	Range resolution	5 m
$V_{max}$	Velocity resolution	5 m/s

### 3.2. Simulation Results of Transmitter

The binary data are generated at the transmitter, and the communication information data are encoded and modulated into the P4 code sequence. After modulation, data are converted into multi-channel low-speed data through series-to-parallel and then IFFT in the digital domain and converted into the serial data stream after parallel-to-serial conversion so as to obtain the carrier signal of IUDCS after OFDM multi-carrier modulation. The in-phase and orthogonal components are shown in Figure 8.

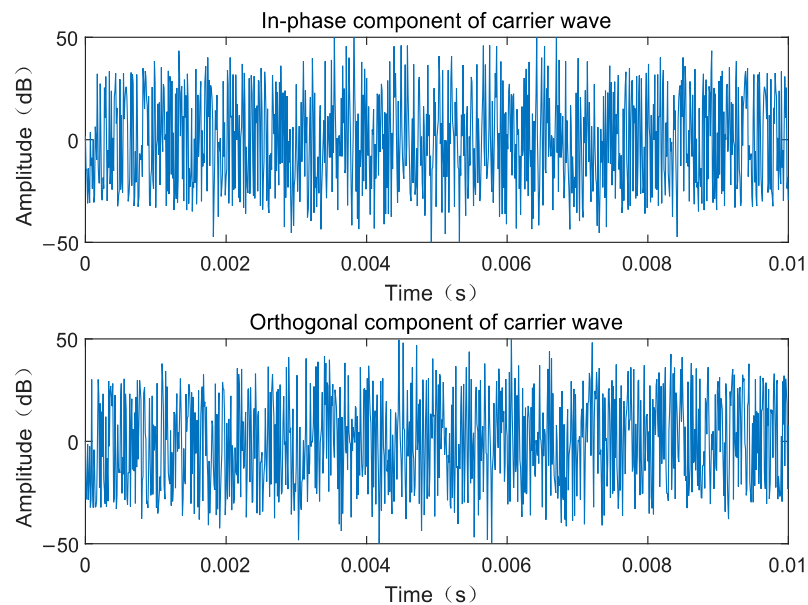


**Figure 8.** In-phase and orthogonal components of the carrier signal for IUDCS.

After OFDM multi-carrier modulation, the serial signal of IUDCS is obtained, and the autocorrelation analysis of the signal is carried out to obtain the simulation results, as shown in Figure 9. The results show that when the length of the intercepted data is consistent with that of the originally transmitted signal, the modulated signal has good autocorrelation. Therefore, while suitable for communication operations, it will reduce the

impact of communication information on detection, which is conducive to the separation of signal and noise, improve the signal-to-noise ratio, and improve the security of system information transmission.

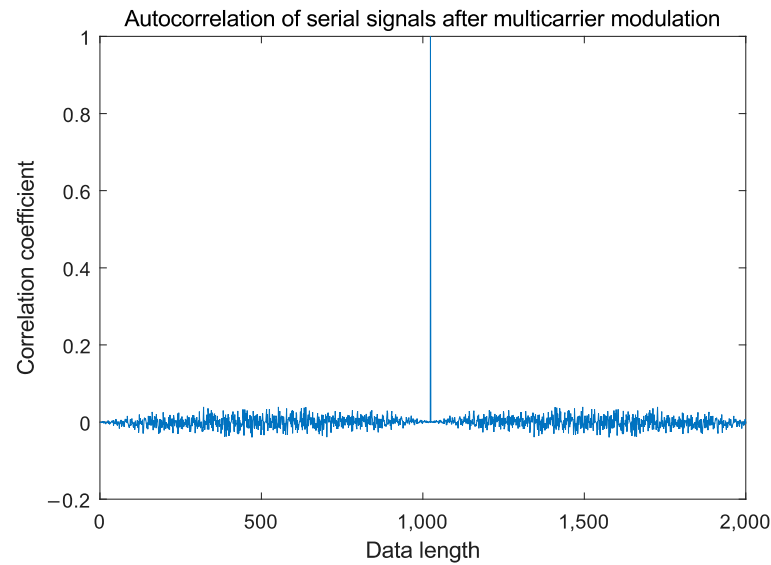


Figure 9. Autocorrelation of signals.

A filter with a normalized cut-off frequency of 1/10 and filter order of 13 is selected to filter the integrated signal of detection and communication after modulation. The output digital signal processed by the digital filter must undergo digital–analog conversion and smoothing processing. The frequency response characteristics of the D/A filter are shown in Figure 10.

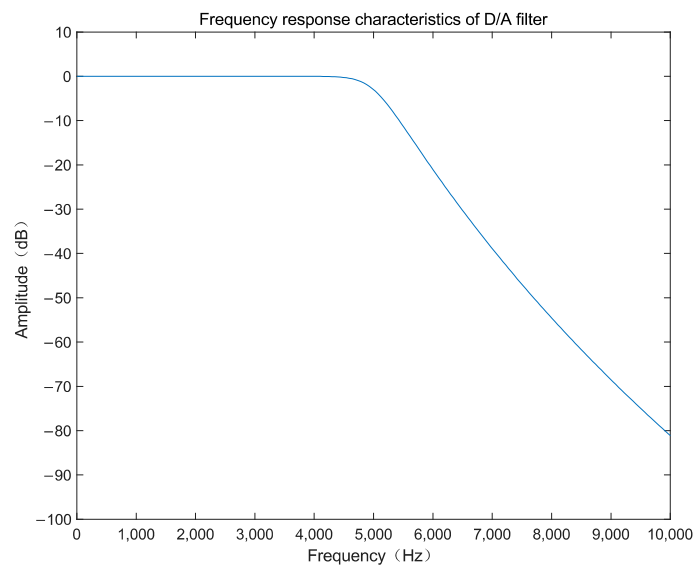
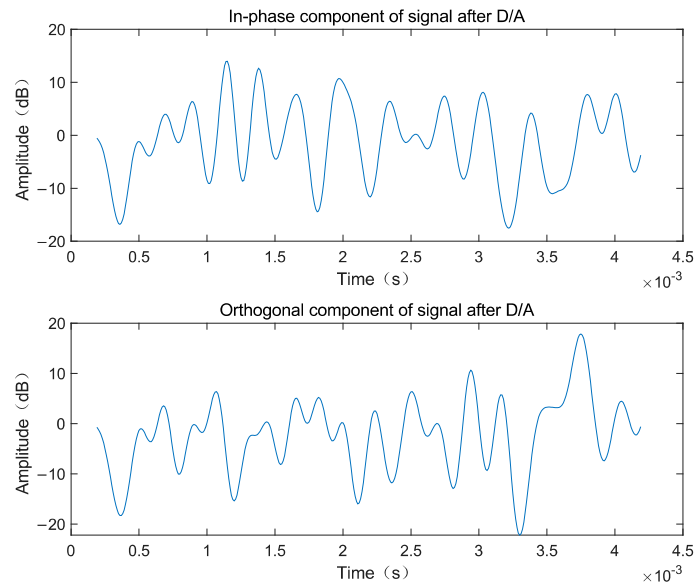


Figure 10. Frequency response characteristics of D/A filter.

The signal data of IUDCS are filtered and smoothed by a D/A filter, and the filtered integrated detection and communication signal transmitted is of the in-phase and orthogonal components, as shown in Figure 11.



**Figure 11.** In-phase and orthogonal components of the signal after filtering.

The filtered in-phase and orthogonal components of the integrated signal of detection and communication are moved to the frequency spectrum to achieve stable underwater operation of the integrated signal and reduce interference. It is easier to obtain high-gain and frequency response characteristics under stable conditions. The in-phase and orthogonal components of the signal of IUDCS are moved to the intermediate frequency, as shown in Figure 12.

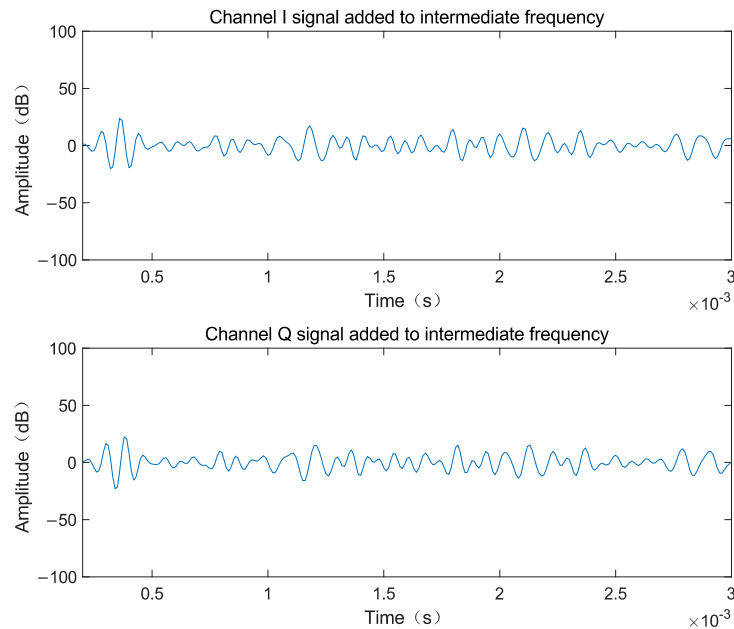


**Figure 12.** Add intermediate frequency signal.

Thus, the transmission signal of IUDCS combined with intermediate frequency output by the underwater transmitting electrode is obtained, and the waveform of the final transmitting terminal is shown in Figure 13.

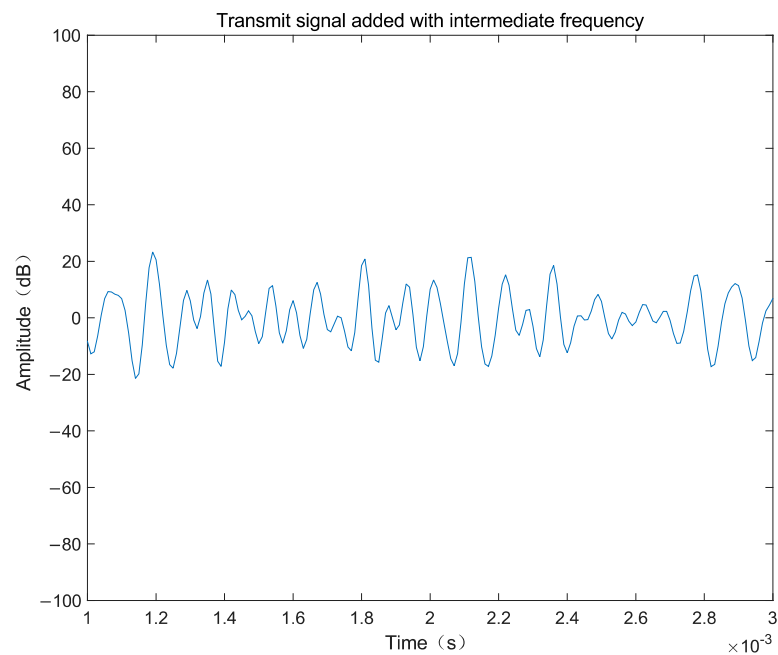


**Figure 13.** Integrated transmission signal of detection communication with intermediate frequency.

### 3.3. Simulation Results of Receiver

Three target information and Gaussian white noise interferences were added to the simulation. The integrated echo signal of detection and communication with the target was obtained at the receiver, as shown in Figure 14.

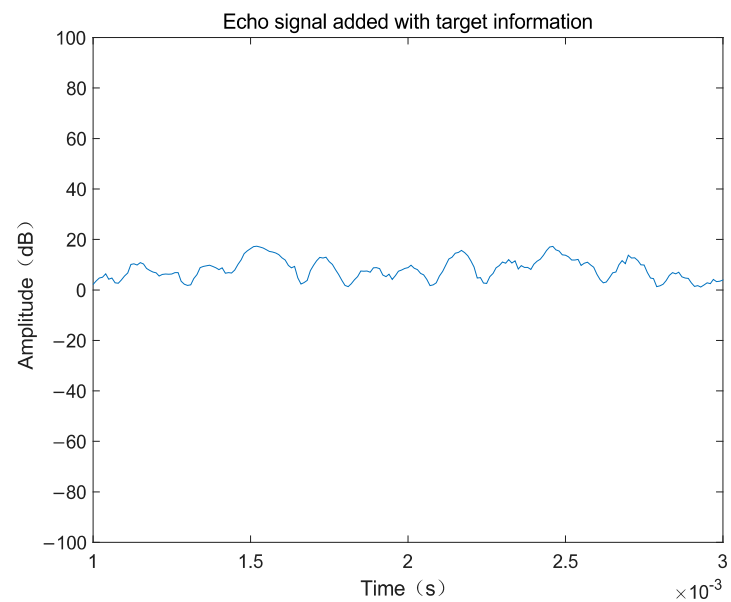


**Figure 14.** Target echo signal.

Then, the detection and communication integrated echo signal added to the target is processed by removing the intermediate frequency. The in-phase and orthogonal components of the detection and communication integrated signal after removing the intermediate frequency are obtained, as shown in Figure 15.

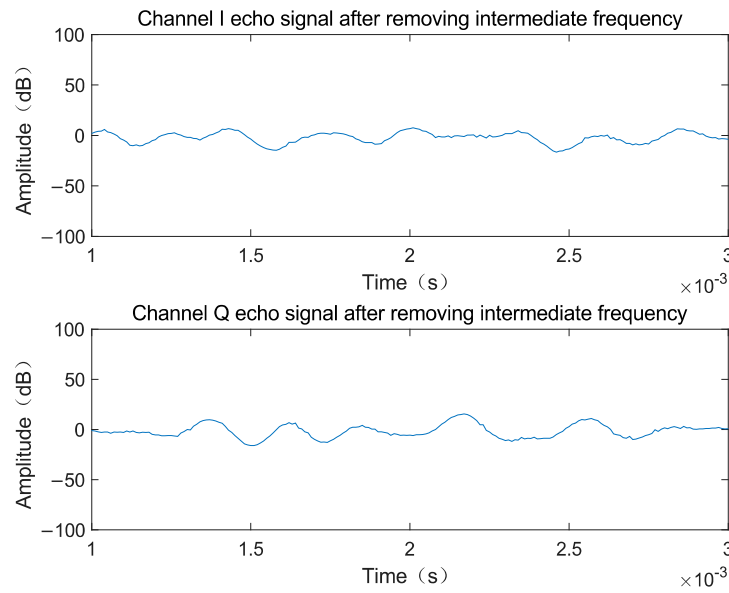


**Figure 15.** Integrated signals of detection and communication after removing intermediate frequency.

Based on the analysis of the integrated sequence of P4 code-modulated OFDM detection and communication, assuming that the integrated system of target distance detection and communication is 10 m, 30 m, and 50 m, and the velocity is 10 m/s, 30 m/s, and 50 m/s, and the channel is a Gaussian white noise channel, the detection processing module completes the identification of target position and speed. Figure 16 simulates the range velocity joint display of the IUDCS echo waveform. It can be seen from the figure that using the pulse compression cascade FFT method can effectively obtain the distance and velocity information of the detected target. The simulation results in Figure 16 show that the dynamic identification of three targets can be achieved. They verify the detection ability of underwater IUDCS signals for targets.

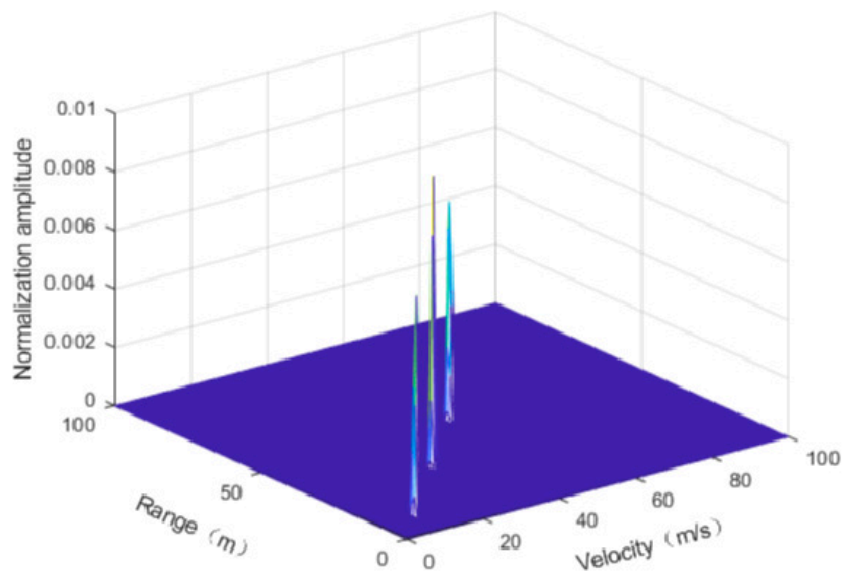


**Figure 16.** Detection signal processing.

Further processes to obtain the detection range and speed output are shown in Figures 17 and 18, respectively.

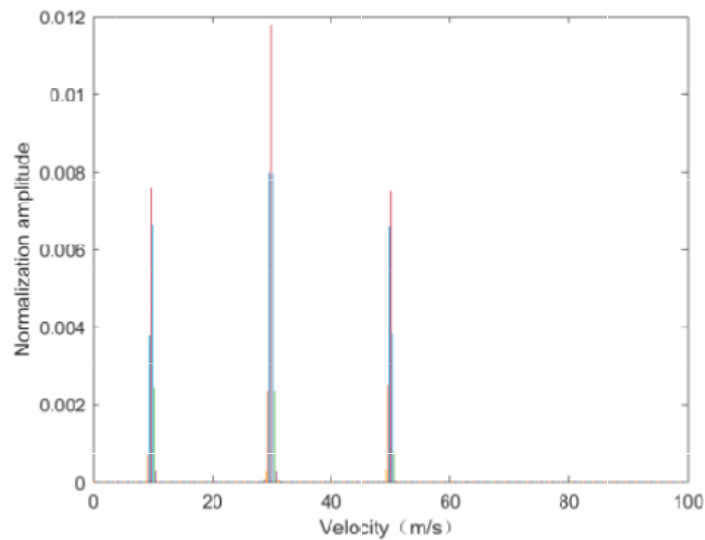


Figure 17. Detection signal velocity output.

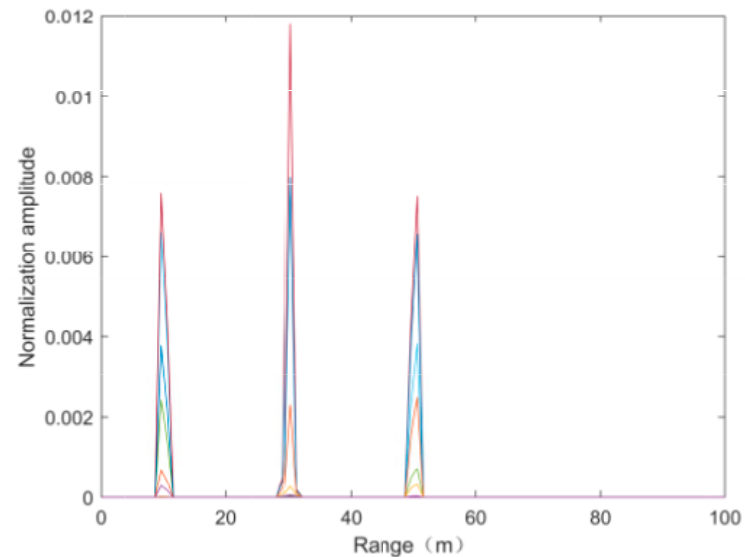
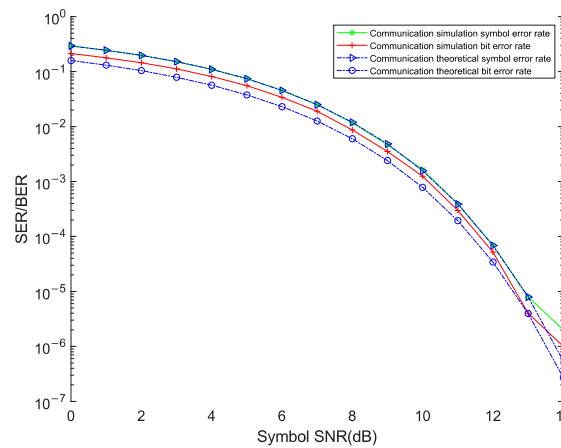


Figure 18. Detection signal range output.

Figure 16 shows the integration of the underwater electric field detection and communication systems based on the OFDM mechanism of the P4 code modulation’s joint display of three target velocities and ranges. As can be seen from Figure 17, the simulation results show that three peaks appear at 10 m, 30 m, and 50 m, respectively, which indicates that the velocity of the three targets has been correctly identified. Similarly, the simulation results show that three peaks appear at 10 m/s, 30 m/s, and 50 m/s, respectively (see Figure 18), which indicates that the range of the three targets has been correctly identified. To sum up, simulation results show that the three dynamic targets have been correctly detected.

The decoding and demodulation process is carried out at the communication end, and the symbol error rate and bit error rate of the integration waveform of the underwater electric field detection and communication system based on the OFDM mechanism of the P4 code modulation are simulated and analyzed. The bit  $N_p$  of P4 code is 32, and the result of the signal received at the receiver of the system is obtained, as shown in Figure 19.



**Figure 19.** Comparison of symbol error rate and bit error rate between communication theory and simulation.

As shown in Figure 17, when the symbol SNR is 0 dB, the symbol error rate of theory and simulation is 0.2921, and the bit error rates are 0.1587 and 0.2125, respectively, in the white Gaussian noise channel. When the symbol SNR is 14 dB, the symbol error rates of theory and simulation are  $5.39 \times 10^{-7}$  and  $4 \times 10^{-6}$ , and the bit error rates are  $2.70 \times 10^{-7}$  and  $0.5 \times 10^{-6}$ , respectively.

The signal bandwidth is  $B$ , and the pulse duration meets  $T_b = N/B$ , where  $N$  represents the number of subcarriers. Since  $N_p = 32$  bit P4 code modulation is adopted, the communication transmission rate can be obtained as follows:

$$q = \frac{\log_2 N_p}{T_b} = \frac{B \cdot \log_2 N_p}{N} = 488.28 \text{ b/s.} \tag{20}$$

The simulation results show that the theory of the symbol error rate and bit error rate of the integrated signal of OFDM detection and communication, modulated by 32-bit P4 code, is consistent with the simulation analysis. Moreover, with the gradual increase of SNR, the symbol error rate decreases by six orders of magnitude, while the bit error rate decreases by five orders of magnitude. The deviation between simulation and theory is due to the threshold effect of phase modulation, so the phase output will be distorted at low SNR. When the symbol SNR is greater than 10 dB, the bit error rate and symbol error rate are both below  $10 \times 10^{-3}$ , which can meet the requirements of underwater electric field communication.

Based on the integrated simulation results of underwater electric field detection and communication, the communication transmission rate is approximately 0.5 kbit/s, which can meet the needs of most underwater electric field close-range communication. When the bandwidth is fixed, increasing the length of the P4 code will reduce the communication rate. Thus, when the symbol signal-to-noise ratio is constant, both the symbol error rate and the bit error rate increase, resulting in a decrease in the effective underwater electric field communication distance. As the transmission frequency of the system signal decreases, the attenuation of the signal in the underwater channel decreases, thereby increasing the transmission range of the channel. However, the lower the transmission frequency, the easier it is for the signal to be submerged by environmental noise, which is not conducive to signal extraction and affects the accuracy of target detection and the communication signal-to-noise ratio. Therefore, in response to the environmental requirements of underwater electric fields, selecting appropriate system parameters such as transmission frequency and P4 code length can achieve the integration of detection and communication systems. The simulation results indicate that the integrated detection and communication system may be applied to unmanned underwater platforms, practicing target detection tasks between clusters.

The current research on the integration of underwater detection and communication mainly focuses on the integration of underwater acoustic systems. The integrated system for electric field detection and communication adopted in this article is still the first to be applied underwater, mainly solving the problems of blind spots in near-field detection and the low connectivity of underwater sound. Advanced technologies such as underwater target recognition based on active low-frequency electric fields and communication between underwater vehicle clusters are adopted. To solve the problems of target detection and mobile communication equipment cluster under complex sea conditions, we realize the multi-resource sharing of underwater cluster equipment, and improve the survivability and adaptability of the system. In the future, the development of an integrated prototype for electric field detection and communication will be completed to verify the system's ability to search for dynamic targets quickly and to communicate signals between clusters without interference and with recognizability.

#### 4. Conclusions

This article proposes an integrated method of underwater electric field detection and communication based on the P4 code-modulated OFDM signal. This method combines detection and communication signals and is applied to underwater electric fields at home and abroad for the first time. The signal form and the waveform representation in the time–frequency domain of the integration of underwater electric field detection and communication systems based on the OFDM mechanism of the P4 code modulation was first given. Then, the target echo model is established. Finally, the integrated signal of OFDM modulated by the P4 code is simulated. The analysis results show that the detection and communication integration system can meet the speed and resolution requirements of the three underwater dynamic targets. Moreover, when the symbol SNR is greater than 10 dB, the bit error rate and symbol error rate are both below  $10 \times 10^{-3}$ , which can meet the requirements of underwater electric field communication. The simulation results verify the detection and communication performance of the underwater electric field IUDCS. This will lay a foundation for the engineering application of IUDCS in subsequent underwater vehicle cluster operation. In the future, we will establish multiple unmanned platforms that integrate detection and communication. By receiving control instructions from the upper computer through a touch platform, integrated signals are transmitted underwater, and other platforms receive signals to complete communication between clusters; they receive cluster operations through multiple platforms to complete tasks such as target encirclement and expulsion. The integrated detection and communication platform has a small size, low energy consumption, and strong maneuverability, making it suitable for covert operations in marine environments. Moreover, electric field communication is less affected by the environment, making it ideal for operations in complex environments such as narrow and dim areas.

**Author Contributions:** Conceptualization, Q.H. and X.F.; methodology, X.F.; software, X.F. and Y.Z.; formal analysis, Q.H.; investigation, X.F. and Z.Z.; writing—original draft preparation, X.F.; writing—review and editing, Q.H., Z.Z. and X.F.; visualization, X.F.; supervision, Q.H., Z.Z. and Y.Z. All authors have read and agreed to the published version of the manuscript.

**Funding:** This research was funded by the Major Program of the National Natural Science Foundation of China, Grant No. 61890961, the General Program of the National Natural Science Foundation of China, Grant No. 61971412, the Basic Research Project of China, Grant No. JCKY2020110C074, and the Rapid Support Fund Project of China, Grant No. 61404150405.

**Institutional Review Board Statement:** Not applicable.

**Informed Consent Statement:** Not applicable.

**Data Availability Statement:** Not applicable.

**Conflicts of Interest:** The authors declare no conflict of interest.

## References

1. Solberg, J.R.; Lynch, K.M.; Maciver, M.A. Active Electrolocation for Underwater Target Localization. *Int. J. Robot. Res.* **2008**, *27*, 529–548. [[CrossRef](#)]
2. Lebastard, V.; Chevallereau, C.; Girin, A.; Servagent, N.; Gossiaux, P.B.; Boyer, F. Environment reconstruction and navigation with electric sense based on a Kalman filter. *Int. J. Robot. Res.* **2013**, *32*, 172–188. [[CrossRef](#)]
3. Morel, Y.; Lebastard, V.; Boyer, F. Neural-based underwater surface localization through electrolocation. In Proceedings of the IEEE International Conference on Robotics and Automation (ICRA), Stockholm, Sweden, 16–21 May 2016; pp. 2596–2603.
4. Lanneau, S.; Lebastard, V.; Boyer, F. Object shape recognition using electric sense and ellipsoid's polarization tensor. In Proceedings of the IEEE International Conference on Robotics and Automation (ICRA), Stockholm, Sweden, 16–21 May 2016; pp. 4692–4699.
5. Lim, H.S.; Ng, B.P.; Reddy, V.V. Generalized MUSIC-Like Array Processing for Underwater Environments. *IEEE J. Ocean. Eng.* **2017**, *42*, 124–134. [[CrossRef](#)]
6. Peng, J.G.; Wu, J. Finite-element simulation study of an underwater active electrolocation system based on Cole-Cole model. *Chin. Sci. Bull.* **2016**, *61*, 2647–2658.
7. Peng, J.; Wu, J. A Numerical Simulation Model of the Induce Polarization: Ideal Electric Field Coupling System for Underwater Active Electrolocation Method. *IEEE Trans. Appl. Supercond.* **2016**, *26*, 0606305. [[CrossRef](#)]
8. Tucker, M.J. Conduction signalling in the sea. *Radio Electron. Eng.* **1972**, *42*, 453–456. [[CrossRef](#)]
9. Momma, H.; Tsuchiya, T. Underwater Communication by Electric Current. In Proceedings of the OCEANS'76, Washington, DC, USA, 13–15 September 1976.
10. Joe, J.; Toh, S.H. Digital Underwater Communication Using Electric Current Method. In Proceedings of the Oceans, Aberdeen, UK, 18–21 June 2007.
11. Kim, C.W.; Lee, E.; Syed, N.A.A. Channel characterization for underwater electric conduction communications systems. In Proceedings of the OCEANS 2010 MTS/IEEE SEATTLE, Seattle, WA, USA, 20–23 September 2010.
12. Wang, W.; Liu, J.; Xie, G.; Wen, L.; Zhang, J. A bio-inspired electrocommunication system for small underwater robots. *Bioinspir. Biomim.* **2017**, *12*, 036002. [[CrossRef](#)] [[PubMed](#)]
13. Zhang, H.; Wang, W.; Zhou, Y.; Wang, C.; Fan, R.; Xie, G. CSMA/CA-based electrocommunication system design for underwater robot groups. In Proceedings of the 2017 IEEE/RSJ International Conference on Intelligent Robots and Systems (IROS), Vancouver, BC, Canada, 24–28 September 2017.
14. Cao, F.; Wang, W.; Xie, G.; Luo, W. Survey of Underwater Electric Field Communication. *Ordnance Ind. Autom.* **2013**, *32*, 51–54.
15. Poncela, J.; Aguayo, M.C.; Otero, P. Wireless Underwater Communications. *Wirel. Pers. Commun.* **2012**, *64*, 547–560. [[CrossRef](#)]
16. Wang, Y.; Zhou, M.; Song, Z. Development of Underwater Wireless Communication Technology. *Commun. Technol.* **2014**, *47*, 589–594.
17. Neveln, I.D.; Bai, Y.; Snyder, J.B.; Solberg, J.R.; Curet, O.M.; Lynch, K.M.; MacIver, M.A. Biomimetic and bio-inspired robotics in electric fish research. *J. Exp. Biol.* **2013**, *216*, 2501–2514. [[CrossRef](#)] [[PubMed](#)]
18. Miller, L.M.; Silverman, Y.; MacIver, M.A.; Murphey, T.D. Ergodic exploration of distributed information. *IEEE Trans. Robot.* **2015**, *32*, 36–52. [[CrossRef](#)]
19. Gottwald, M.; Herzog, H.; von der Emde, G. A bio-inspired electric camera for short-range object inspection in murky waters. *Bioinspir. Biomim.* **2019**, *14*, 035002. [[CrossRef](#)] [[PubMed](#)]
20. Zhou, Y.; Wang, W.; Zhang, H.; Zheng, X.; Li, L.; Wang, C.; Xu, G.; Xie, G. Underwater robot coordination using a bio-inspired electrocommunication system. *Bioinspir. Biomim.* **2022**, *17*, 056005. [[CrossRef](#)] [[PubMed](#)]
21. Blouin, S.; Lucas, C. Early Results and Description of an Underwater Electric-field Sensing and Communication Experiment in Bedford Basin. In Proceedings of the 2022 IEEE Canadian Conference on Electrical and Computer Engineering (CCECE), Halifax, NS, Canada, 18–20 September 2022; pp. 28–32.
22. Rong, S. Unification Analysis on Communication Equation and Radar Equation. *Electron. Warf.* **2006**, *4*.
23. Qiang, L.I.; Jie, W. Joint wireless communication and radar sensing: Review and future prospects. *J. Signal Process.* **2020**, *36*, 1615–1627.
24. Wang, M. *Research on the Design of Integrated Signal for Radar and Communication Based on OFDM*; Xidian University: Xi'an, China, 2015.
25. Liu, Z.; Zhang, Y.; Luo, X. Performance Analysis of Radar Communication Shared Signal Based on OFDM. In Proceedings of the International Conference on Communications and Networking in China, Virtual Event, 21–22 November 2021; Springer: Cham, Switzerland, 2022; pp. 250–263.
26. Mohseni, R.; Sheikhi, A.; Masnadi-Shirazi, M.A. Multicarrier constant envelope OFDM signal design for radar applications. *AEU-Int. J. Electron. Commun.* **2010**, *64*, 999–1008. [[CrossRef](#)]
27. Peng, J.; Sheng, W.G.; Yuan, X.H. Bandlimited Effects on Digital Polyphase Coded Pulse Compressors in the receiver. *Radar Ecm.* **2002**, *4*, 30–33.
28. Zhang, H. *Waveform Design and Performance Analysis of Integrated Radar Communication*; Harbin Engineering University: Harbin, China, 2021.
29. Koopman, P. 32-bit cyclic redundancy codes for internet applications. In Proceedings of the International Conference on Dependable Systems and Networks, Washington, DC, USA, 23–26 June 2002; pp. 459–468.
30. Indumathi, G.; Ananthakirupa, V.A.A.; Ramesh, M. Architectural design of 32 bit polar encoder. *Circuits Syst.* **2016**, *7*, 551. [[CrossRef](#)]

31. Thompson, S.C.; Ahmed, A.U.; Proakis, J.G.; Zeidler, J.R.; Geile, M.J. Constant Envelope OFDM. *IEEE Trans. Commun.* **2008**, *56*, 1300–1312. [[CrossRef](#)]
32. Ahmed, A.U.; Thompson, S.C.; Zeidler, J.R. Constant envelope OFDM with channel coding. In Proceedings of the MILCOM 2006–2006 IEEE Military Communications Conference, Washington, DC, USA, 23–25 October 2006; pp. 1–7.
33. Zheng, J. *Study on Some Key Issues of OFDM Wireless Communication System*; University of Electronic Science and Technology of China: Chengdu, China, 2010.
34. He, J. *Design of Radar Communication Integrated Signal Based on OFDM*; University of Electronic Science and Technology of China: Chengdu, China, 2017.
35. Liang, T.; Li, Z.; Wang, M.; Fang, X. Design of radar-communication integrated signal based on OFDM. In Proceedings of the International Conference on Artificial Intelligence for Communications and Networks, Harbin, China, 25–26 May 2019; Springer: Cham, Switzerland, 2019; pp. 108–119.

**Disclaimer/Publisher’s Note:** The statements, opinions and data contained in all publications are solely those of the individual author(s) and contributor(s) and not of MDPI and/or the editor(s). MDPI and/or the editor(s) disclaim responsibility for any injury to people or property resulting from any ideas, methods, instructions or products referred to in the content.